sustainability

MDPI

Article

Thermodynamic Analysis of the Solubility of Propylparaben in Acetonitrile–Water Cosolvent Mixtures

Claudia Patricia Ortiz [1], Rossember Edén Cardenas-Torres [2], Mauricio Herrera [3] and Daniel Ricardo Delgado [3,*]

[1] Programa de Administración en Seguridad y Salud en el Trabajo, Grupo de Investigación en Seguridad y Salud en el Trabajo, Corporación Universitaria Minuto de Dios-UNIMINUTO, Neiva 410001, Colombia
[2] Grupo de Fisicoquímica y Análisis Matemático, Facultad de Ciencias y Humanidades, Fundación Universidad de América, Avenida Circunvalar No. 20-53, Bogotá 111221, Colombia
[3] Programa de Ingeniería Civil, Grupo de Investigación de Ingenierías UCC-Neiva, Facultad de Ingeniería, Universidad Cooperativa de Colombia, Sede Neiva, Neiva 410001, Colombia
* Correspondence: danielr.delgado@campusucc.edu.co; Tel.: +57-3219104471

Abstract: Parabens are substances used in the food, pharmaceutical and cosmetic industries. Recent studies have indicated that these substances have toxic potential, cause endocrine disruption and can easily bioaccumulate; therefore, their physicochemical properties are of industrial, biological and environmental interest. Due to their potential use in the development of more efficient and cleaner processes, the design of environmental recovery strategies and more reasonable designs for solubility in cosolvent mixtures, studies of thermodynamic analysis and mathematical modeling are of great interest. This research studies the solubility of propylparaben in acetonitrile + water cosolvent mixtures at nine temperatures by UV/Vis spectrophotometry, analyzing the solid phase by differential scanning calorimetry to evaluate possible polymorphic changes. The solubility of propylparaben is an endothermic process, where phase separation occurs at intermediate mixtures, reaching its minimum solubility in pure water at 278.15 K and the maximum solubility in pure acetonitrile at 315.15 K. The experimental data are well-correlated with the va not Hoff, Apelblat and Buchowski–Ksiazaczak models. The results revealed that possible microheterogeneity of the MeCN + W mixture can generate phase separation in intermediate mixtures, possibly due to the formation of solvates or hydrates.

Keywords: propylparaben; solubility; water; acetonitrile; solution; thermodynamics; cosolvent mixtures

Citation: Ortiz, C.P.; Cardenas-Torres, R.E.; Herrera, M.; Delgado, D.R. Thermodynamic Analysis of the Solubility of Propylparaben in Acetonitrile–Water Cosolvent Mixtures. *Sustainability* **2023**, *15*, 4795. https://doi.org/10.3390/su15064795

Academic Editor: Agostina Chiavola

Received: 6 February 2023
Revised: 28 February 2023
Accepted: 3 March 2023
Published: 8 March 2023

1. Introduction

Propylparaben (PP), ($C_{10}H_{12}O_3$, CAS Number: 94-13-3, Figure 1) is a propyl ester of parahydroxybenzoic acid that is widely used in the pharmaceutical, cosmetic and food industries due to its low toxicity and broad antibacterial and antifungal spectrum over a wide pH range [1–4].

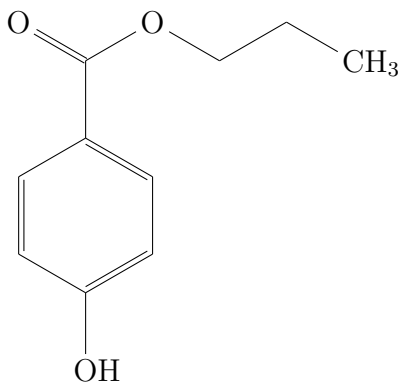

Figure 1. Molecular structure of the propylparaben (propyl 4-hydroxybenzoate) [5].

Due to the low solubility of PP in water, solubility studies in organic solvents and cosolvent mixtures are crucial lines of research. These studies aim to devise strategies to improve PP solubility, considering the importance of this physicochemical property in processes, such as recrystallization, purification, quality analysis, quantification, preformulation studies and pharmaceutical dosage design [6–10].

Regarding environmental factors, solubility data allow for the design of more efficient processes, which means a reduction in waste and, therefore, a reduction in environmental impact, which is an issue that has become highly relevant and where many researchers have focused their attention [11,12]. In addition, some environmental parameters are calculated from the solubility data, such as Abraham parameters, which are used for the calculation of the lethal median molar concentration, bioaccumulation analysis and partitioning processes [13,14].

Cosolvency is one of the main strategies used to increase the solubility of poorly water-soluble drugs since the addition of an organic solvent miscible with water can favor water destructuration. This reduces the "squeezing out" effect, in addition to reducing the polarity of the cosolvent system, thereby, favoring non-polar interactions [15–18].

One of the most widely used cosolvent mixtures in the pharmaceutical industry is {acetonitrile (MeCN) + water (W)} [19,20]. MeCN is an aprotic polar solvent, miscible with water in all proportions and used to dissolve semipolar substances, which theoretically makes it a suitable choice to develop aqueous mixtures, which are widely used in HPLC. On the other hand, water is the green solvent par excellence, and water solubility data are highly relevant in the development of pharmaceutical products [7].

Broadly speaking, solubility data are the baseline for many industrial processes and the key to understanding the design of pharmaceuticals and cosmetics. Therefore, solubility studies are essential to the industry for routine process development, quantification, quality control and for research and development purposes. The aim of this research was to thermodynamically analyze the solubility of PP in cosolvent mixtures {MeCN (1) + W (2)} at nine temperatures, where one of the most relevant results was the separation of liquid phases in intermediate cosolvent mixtures.

2. Materials and Methods

2.1. Materials

For the development of the research, propylparaben (PP) (purity > 0.990, CAS: 57-83-0, Sigma-Aldrich, Burlington, VT, USA) was used as the study drug and defined as compound **3**; two solvents were also used, acetonitrile (MeCN) (purity > 0.998 CAS: 75-05-8, Merck Millipore, Burlington, VT, USA) defined as compound **1** and water (W) defined as compound **2**.

2.2. Preparation of Solvent Mixtures

Nineteen cosolvent mixtures {MeCN (1) + W (2)} from 0.05 up to 0.95 in MeCN mass fraction were prepared in 15 mL capacity amber bottles using an analytical balance (RADWAG AS 220.R2, Torun, Poland) of four decimal places with a sensitivity of ±0.0001 g. Three samples of approximately 10.00 ± 0.00 g were prepared for each of the concentrations.

2.3. Solubility Determination

The determination of PP solubility in mixtures {MeCN (1) + W (2)} was performed following the protocol of the shake-flask method proposed by Higuchi and Connors [21–23]. The method was developed in three steps:

1. Sample saturation: PP was added to each of the cosolvent mixtures {MeCN (1) + W (2)} until a saturated solution in equilibrium with the solid phase was obtained. The samples were subjected to ultrasound for 30 min and then placed in a recirculating water bath (thermostat) at each of the study temperatures (278.15, 283.15, 288.15, 293.15, 298.15, 303.15, 308.15, 313.15 and 318.15 K) for a period of 72 h (a constant concentration was verified).
2. Phase separation: The filtration method was employed using membranes with a pore diameter of 0.45 µm (Millipore Corp. Swinnex, Burlington, VT, USA). Using a syringe previously thermostatted to the study temperature, an aliquot of the supernatant was taken and then poured through the membrane. In order to reduce the possible effects of solute sorption on the filter membrane, the first drops of the filtrate were discarded.
3. Saturated solution and solid phase analysis: The concentration of PP in each of the samples was determined by UV/Vis spectrophotometry. From the filtered aliquot, gravimetric dilutions were performed with NaOH 0.1 N (NaOH 0.1 N was used since mixing the saturated solution with the NaOH solution forms the sodium salt of PP, and as the salt is very soluble in aqueous media, the probability of PP precipitation decreases). After dilution, the samples were analyzed in a UV/Vis spectrophotometer UV/Vis (UV/VIS EMC-11- UV spectrophotometer, Dresden, Germany) at 256 nm (the wavelength of maximum absorbance) for the prior construction of the calibration curve. In order to identify possible polymorphic changes, solid samples in equilibrium were analyzed using differential scanning calorimetry (DSC) and X-ray powder diffraction (XRPD).

3. Results and Discussion

3.1. Solubility (x_3) of Propylparaben (3) in 10 Cosolvent Mixtures {Acetonitrile (1) + Water (2)}

Table 1 shows the solubility of PP (3) in cosolvent mixtures {MeCN (1) + W (2)} (Figure 2). In each case, the solubility of PP increases with increasing temperature suggesting an endothermic process. Furthermore, as the concentration of MeCN in the system increases from pure water to $w_1 = 0.20$, the solubility of PP increases, and from $w_1 = 0.20$ up to $w_1 = 0.80$, a separation of liquid phases is observed. The latter is possibly due to a higher affinity of PP for one of the solvents in the mixture (MeCN or W), which would disfavor the solvent–solvent interaction generating phase separation. Moreover, the mixture {MeCN (1) + W (2)} exhibits microheterogeneity in intermediate mixtures [24,25], which could be an additional factor contributing to phase separation.

This phenomenon has also been reported by other authors in solubility studies of parabens in the same cosolvent system. Romero-Nieto et al. reports phase separation in solubility studies of methylparabens [19] and ethylparabens [20] in cosolvent mixtures {MeCN (1) + W (2)}. Paruta et al. and Yang and Rasmuson also reported phase separation in solubility studies of parabens in cosolvent mixtures {dioxane (1) + water (2)} [26] and {ethanol (1) + water (2)} [3]; and Peña et al. and Paruta et al. have also reported this in solubility studies of other drugs, such as benzocaine, salicylic acid and xanthines in mixtures {dioxane (1) + water (2)} [27,28].

Within $w_1 = 0.80$ to $w_1 = 1.0$ cosolvent concentration range, the PP solubility increases from $w_1 = 0.80$ up to $w_1 = 0.90$, where the maximum solubility is reached; and from

$w_1 = 0.90$ to pure MeCN, the PP solubility decreases indicating a negative cosolvent effect of MeCN within this range of concentration. According to Hildebrand, the maximum solubility is reached in cosolvent mixtures where the solubility parameter of the drug is similar to that of the cosolvent system [29].

In this case, the solubility parameter of PP is 25.4 $MPa^{1/2}$ [4], and that of the cosolvent mixture ($w_1 = 0.9$) is 28.99 $MPa^{1/2}$ [20], thus, showing the utility of Hildebrand's theory when choosing solvents or cosolvent mixtures to improve the solubility of a substance.

Table 1. Experimental solubility of propylparaben (3) in {acetonitrile (1) + water (2)} cosolvent mixtures expressed as a mole fraction ($10^4 x_3$) at different temperatures and $p = 96$ kPa [a,c].

w_1 [b]	Temperatures								
	278.15	**283.15**	**288.15**	**293.15**	**298.15**	**303.15**	**308.15**	**313.15**	**318.15**
0.00	0.1468	0.1873	0.2176	0.2804	0.3422	0.4265	0.5617	0.7132	0.842
0.05	0.1498	0.1995	0.2502	0.3121	0.3849	0.4743	0.5856	0.7717	0.8939
0.10	0.1603	0.2013	0.2543	0.343	0.4307	0.533	0.6699	0.8298	1.0109
0.15	0.1771	0.2149	0.2625	0.365	0.4679	0.5712	0.698	0.8956	1.1508
0.20	0.2053	0.2819	0.3545	0.4612	0.6085	0.7737	0.9582	1.2116	1.5053
0.80	387.3	502.2	631.8	813.6	959.2	1224.4	1527.4	1934.9	2238.3
0.85	419.9	576.8	741.8	1053.1	1342.9	1723.9	2322.8	3019.9	3642.3
0.90	438.0	613.2	795.4	1118.4	1477.2	1925.1	2535.5	3365.1	4148.8
0.95	429.5	572.0	786.6	1019.1	1364.4	1765.4	2363.6	2966.9	3804.4
1.00	403.2	516.1	693.4	817.8	1058.8	1373.0	1877.7	2115.1	2834.2

[a] The atmospheric pressure in Neiva, Colombia. [b] The mass fraction of acetonitrile (1) in the acetonitrile (1) + water (2) mixtures free of propylparaben (3). [c] The standard uncertainty in p is $u(p) = 3.0$ kPa. The average relative standard uncertainty in w_1 is $u_r(w_1) = 0.0008$. The standard uncertainty in T is $u(T) = 0.10$ K. The average relative standard uncertainties in x_3 is $u_r(x_{3(1+2)}) = 0.025$.

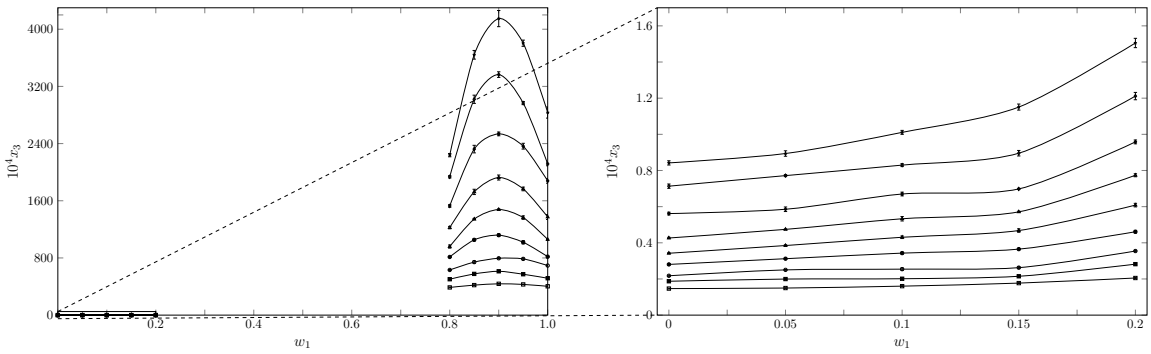

Figure 2. Solubility of propylparaben(3) ($10^4 x_3$) in MeCN (1) + W (2) cosolvent mixtures vs. the mass fraction of MeCN at nine temperatures (□: n278.15 K; ■: 283.15 K; ○: 288.15 K; ●: 293.15 K; ▲: 298.15 K; △: 303.15 K; ♦: 308.15 K; ◊: 313.15 K; and +: 318.15 K).

When comparing the solubility data in water with those reported by other authors, a good match is observed with the data given by Alexander et al. [30], which present relative deviations between 2% and 8% (RD $= |100(x_3 - x_3^R)/x_3|$, where x_3 is the data reported in this paper, and x_3^R is that reported in the literature). Furthermore, when comparing with the data reported by Prankerd [31], the most significant differences were found at 313.15 and 318.15 K, with RDs of 19% and 12%, respectively. At other temperatures, the RDs were between 2% and 8%. Regarding the data reported by Yang and Rasmuson [32], at 313.15 K, there is a significant difference with an RD of 42.9%.

Finally, the MeCN solubility data were compared with those reported by Ouyang et al. [33], and RDs between 23% and 31% were observed. These differences may be due to different equilibrium times, PP water content when preparing the sample, among other experimental factors. An important factor in drug solubility studies is the analysis of

the solid phase in equilibrium with different cosolvent compositions in order to identify possible polymorphic changes.

Differential scanning calorimetry (DSC) and X-ray powder diffraction (XRPD) analyses of the commercial sample and three samples of solid phases in equilibrium with water ($w_1 = 0.80$) and MeCN are presented in Figures 3 and 4. According to the DSC analysis (Table 2), PP does not show polymorphic transitions, since in each case, both the temperature and enthalpy of melting are similar. When comparing the DSC analysis results with the data reported in the literature, good similarity between the data is observed.

In order to verify the calorimetric analysis results, an XRPD analysis was performed (Figure 4), where for each of the four samples, six well-defined peaks at 10, 11, 16, 24, 25 and 33 2θ degrees were found, indicating that there were no polymorphic changes. This is consistent with the results reported by Rudyanto et al. [5] and Yang et al. [34], and it can be observed that the patterns match in the number of peaks. However, the relative intensity varies, possibly due to the way the sample was prepared—in particular, the homogenization process.

Table 2. The thermophysical properties of propylparaben obtained by DSC.

Sample	Enthalpy of Melting, $\Delta_m H$/kJ·mol^{-1}	Melting Point T_m/K
Original sample	27.0 ± 0.5	369.6 ± 0.5
	26.150 [a]	369.7 [a]
	27.9 ± [b]	369.5 ± 0.5 [b]
	28.4 ± 0.6 [c]	369.4 ± 0.5 [c]
	27.2 ± 0.8 [d]	369.4 ± 0.5 [d]
	28.0 [e]	369.65 [e]
	26.51 [f]	369.6 [f]
	24.75 [g]	370.92 [g]
Water	26.8 ± 0.5	369.4 ± 0.5
$w_{0.80}$	27.1 ± 0.5	369.9 ± 0.5
Acetonitrile	26.9 ± 0.5	370.1 ± 0.5

[a] Martin and Carstensen [35]. [b] Ouyang et al. [33]. [c] Cárdenas et al. [4]. [d] Perlovich et al. [36]. [e] Prankerd [31]. [f] Giordano et al. [37]. [g] Rudyanto et al. [5].

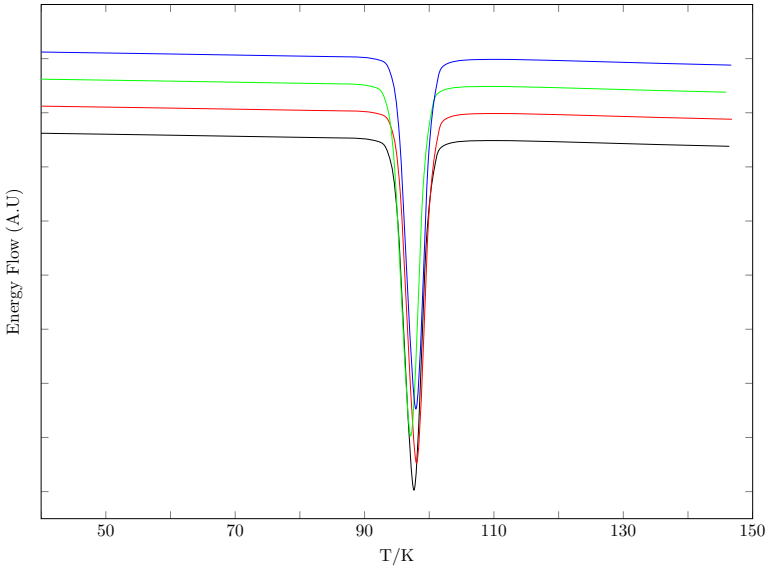

Figure 3. DSC of the equilibrium solid phase of propylparaben (blue: MeCN; green: w_1 = 0.80; red: W; and black: original sample).

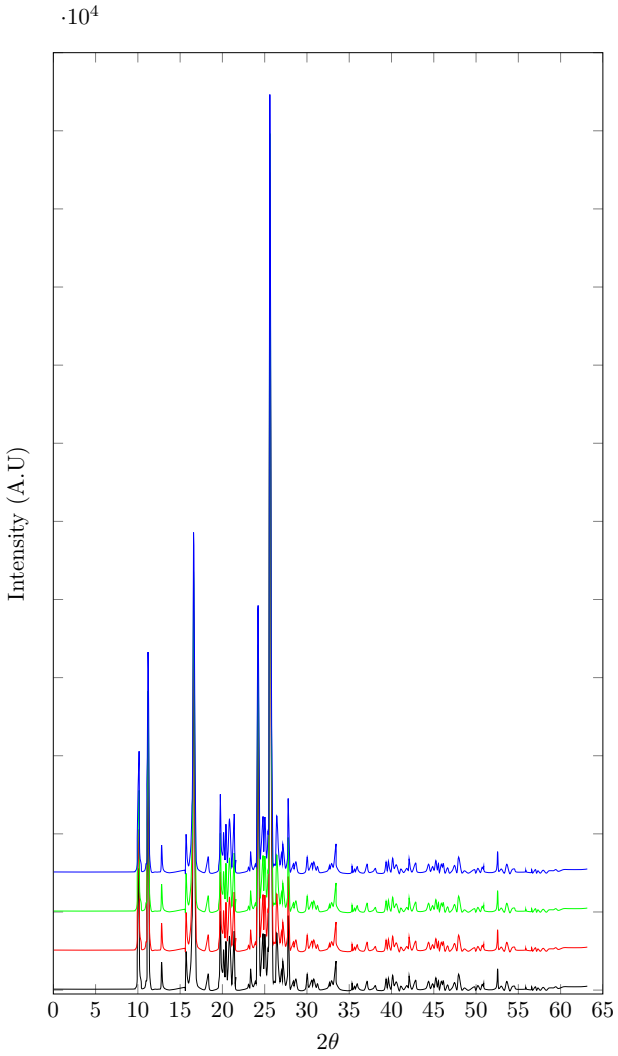

Figure 4. XRPD patterns of propylparaben samples (blue: MeCN; green: w_1 = 0.80; red: W; and black: original sample).

3.2. Thermodynamic Functions of Solution

The solution thermodynamic functions were calculated from the experimental solubility data (Table 1) by the Gibbs–va not Hoff–Krug Equations [38,39] (Equations (1)–(3)).

$$\Delta_{\text{soln}}H^{\circ} = -R\left(\frac{\partial \ln x_3}{\partial\left(T^{-1} - T_{\text{hm}}^{-1}\right)}\right)_p \tag{1}$$

$$\Delta_{\text{soln}}G^{\circ} = -RT_{\text{hm}} \cdot \text{intercept} \tag{2}$$

$$\Delta_{\text{soln}}S^{\circ} = (\Delta_{\text{soln}}H^{\circ} - \Delta_{\text{soln}}G^{\circ})T_{\text{hm}}^{-1} \tag{3}$$

$$T_{\text{hm}} = \frac{n}{\sum_{i=1}^{n}\left(\frac{1}{T}\right)} \tag{4}$$

$$\zeta_H = \frac{|\Delta_{\text{soln}}H^{\circ}|}{|\Delta_{\text{soln}}H^{\circ}| + |T\Delta_{\text{soln}}S^{\circ}|} \tag{5}$$

$$\zeta_{TS} = 1 - \zeta_H \quad (6)$$

where $\Delta_{soln}H^\circ$, $\Delta_{soln}G^\circ$ and $\Delta_{soln}S^\circ$ are the thermodynamic functions of enthalpy, the Gibbs energy and entropy of solution (in kJ mol^{-1}), x_3 is the solubility as a mole fraction, T is the temperature (in K), T_{hm} is the harmonic mean for n study temperatures (in K), R is the molar gas constant (in J K^{-1} mol^{-1}), "intercept" is the intercept of each equation in the va not Hoff plot, and ζ_H and ζ_{TS} are the relative contributions of the enthalpy and entropy of solution to the Gibbs energy.

Following the va not Hoff–Krug model, the enthalpy (Equation (1)) and Gibbs energy (Equation (2)) of solution were calculated from the slope and the intercept of the equation that describes the behavior of the logarithm of solubility as a function of the inverse of temperature ($T^{-1} - T_{hm}^{-1}$).

As shown in Table 3, the Gibbs energy is positive for each case and decreases from pure water to the $w_1 = 0.2$ mixture. Within the $w_1 = 0.2$ up to the $w_1 = 0.8$ cosolvent concentration range, no values were reported due to the liquid phase separation. Between $w_1 = 0.8$ and $w_1 = 0.9$, the $\Delta_{soln}G^\circ$ continuously decreases as a consequence of the increasing solubility; and from $w_1 = 0.9$ up to pure MeCN, there is an increase due to a solubility decrease as a consequence of adding MeCN to the mixture.

Table 3. Thermodynamic functions of propylparaben solution process (3) in {acetonitrile (1) + water (2)} cosolvent mixtures at $T_{hm} = 297.6$ K [a].

w_1 [b]	$\Delta_{soln}G^\circ$/ (kJ·mol^{-1})	$\Delta_{soln}H^\circ$ (kJ·mol^{-1})	$\Delta_{soln}S^\circ$ (J·mol^{-1}·K^{-1})	$T_{hm}\Delta_{soln}S^\circ$ (kJ·mol^{-1})	ζ_H [c]	ζ_{TS} [c]
0.00	25.37	32.62	24.35	7.25	0.818	0.182
0.05	25.17	32.70	25.30	7.53	0.813	0.187
0.10	24.97	34.36	31.57	9.40	0.785	0.215
0.15	24.79	34.76	33.51	9.97	0.777	0.223
0.20	24.12	36.47	41.48	12.34	0.747	0.253
0.80	5.77	32.50	89.83	26.73	0.549	0.451
0.85	5.03	40.23	118.28	35.2	0.533	0.467
0.90	4.82	41.65	123.76	36.83	0.531	0.469
0.95	5.00	40.29	118.60	35.29	0.533	0.467
1.00	5.52	35.67	101.32	30.15	0.542	0.458

[a] The average relative standard uncertainty in w_1 is $u_r(w_1) = 0.0008$. The standard uncertainty in T is $u(T) = 0.10$ K. The average relative standard uncertainty in apparent thermodynamic quantities of real dissolution processes are $u_r(\Delta_{soln}G^\circ) = 0.017$, $u_r(\Delta_{soln}H^\circ) = 0.020$, u_r ($\Delta_{soln}S^\circ$) = 0.022, and $u_r(T\Delta_{soln}S^\circ)$ = 0.022. [b] w_1 is the mass fraction of acetonitrile (1) in the {acetonitrile (1) + 1-propanol (2)} mixtures free of propylparaben (3). [c] ζ_H and ζ_{TS} are the relative contributions by enthalpy and entropy toward the apparent Gibbs energy of dissolution.

The $\Delta_{soln}H^\circ$ increases from pure water up to $w_1 = 0.2$. Generally, in hydroalcoholic mixtures, this increase in water-rich mixtures is due to the water molecules destructuring around the non-polar groups of the drug [40]. However, in {MeCN (1) + W (2)} mixtures, MeCN works as a structuring agent for water molecules; thus, in this case, the enthalpy increase is possibly due to a breakdown in PP molecules.

From $w_1 = 0.8$ up to $w_1 = 0.9$, the solution enthalpy increases and then decreases from $w_1 = 0.9$ up to pure MeCN. When analyzing the behavior of $\Delta_{soln}S^\circ$, it is positive in all cases, thus, favoring the PP solution process. The solution entropy increases from pure water up to $w_1 = 0.2$ and from $w_1 = 0.8$ up to $w_1 = 0.9$, indicating a positive cosolvent effect of MeCN. From $w_1 = 0.9$ up to pure MeCN, the $\Delta_{soln}S^\circ$ decreases, thereby, reducing the entropic benefit.

Finally, by using the results obtained from Equations (5) and (6), the relative contributions of enthalpy (energy factor) and entropy (organizational factor) were identified. Accord-

ing to the values shown in Table 3, ζ_H presents values higher than 0.5 in each case, indicating that the solution enthalpy contributes in a high proportion to the PP solution process.

3.3. Thermodynamic Functions of Mixing

The solution process involves breaking and forming bonds (Figure 5). Initially, the solute and solvent molecules must disperse, then the solute must change state, and finally the solvent molecules must restructure to form the cavity that will host the solute molecule. In both cases, energy must be supplied, and thus these sub-processes are highly endothermic and, therefore, energetically unfavorable for the solution process. Once both solute and solvent molecules are dispersed, the mixing process takes place, and the solution is formed [41].

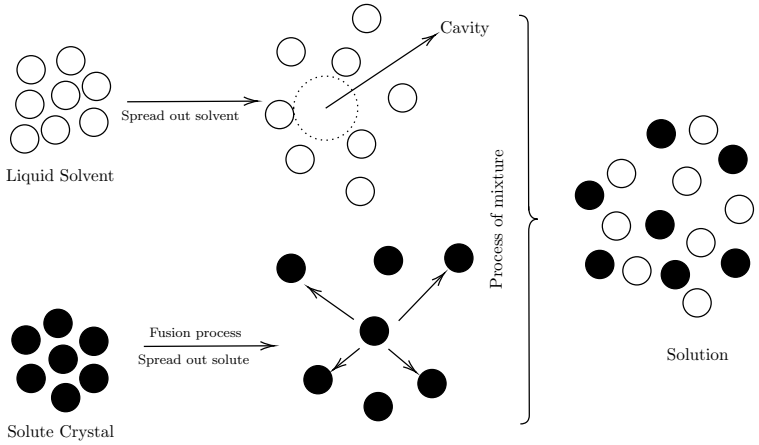

Figure 5. Diagram of the solution processes.

Mathematically, the solution process can be expressed as follows [42]:

$$\Delta_{\text{soln}} f^{\circ} = \Delta_{\text{m}} f^{\circ} + \Delta_{\text{mix}} f^{\circ} \tag{7}$$

where f stands for thermodynamic functions (Gibbs energy, enthalpy or entropy), and the subscripts **m** and **mix** refer to the melting and mixing processes, respectively.

From Equation (7), $\Delta_{\text{mix}} f^{\circ}$ is solved, obtaining Equation (8).

$$\Delta_{\text{mix}} f^{\circ} = \Delta_{\text{soln}} f^{\circ} - \Delta_{\text{m}} f^{\circ} \tag{8}$$

In this work, the thermodynamic melting functions were replaced by the ideal process thermodynamic functions, calculated from the ideal solubility (Table 4) by Equation (9).

$$\ln x_3^{id} = -\frac{\Delta_{\text{m}} H}{R}\left(\frac{T_{\text{m}} - T}{T_{\text{m}} T}\right) + \frac{\Delta C_p}{R}\left(\frac{T_{\text{m}} - T}{T}\right) - \frac{\Delta C p}{R}\ln\left(\frac{T_{\text{m}}}{T}\right) \tag{9}$$

where T and T_{m} are the study temperature and the melting temperature, respectively (in K), $\Delta_{\text{m}} H$ is the melting enthalpy (in kJ mol^{-1}) of the solute, R is the gas constant (in kJ mol^{-1}K^{-1}), and ΔC_p is the differential heat capacity of melting (in kJ K^{-1}mol^{-1}) [43]. Some researchers, such as Hildebrand [29], Neau and Flynn [44], Neau et al. [45] and Opperhuizen et al. [46], assume ΔC_p as the entropy of melting ($\Delta_{\text{m}} S$), which is calculated as $\Delta_{\text{m}} H / T_{\text{m}}$.

According to the thermodynamic functions shown in Table 5, in water-rich mixtures (from pure water up to $w_1 = 0.2$), the Gibbs energy is positive and decreases as the MeCN concentration increases, thereby, indicating a lower energy requirement for cavity formation [47]. Within this cosolvent concentration range, enthalpic (+) and entropic (−) disfavor is observed.

Table 4. Solubility and thermodynamic functions of the PP ideal solution process.

Variable	Temperatures								
	278.15	**283.15**	**288.15**	**293.15**	**298.15**	**303.15**	**308.15**	**313.15**	**318.15**
IS [a]	0.1468	0.1873	0.2176	0.2804	0.3422	0.4265	0.5617	0.7132	0.842
$\Delta_{\mathbf{Soln}}G^{\mathbf{Id}}$ [b]	4.84 kJ·mol^{-1}								
$\Delta_{\mathbf{Soln}}H^{\mathbf{Id}}$	22.45 kJ·mol^{-1}								
$\Delta_{\mathbf{Soln}}S^{\mathbf{Id}}$	59.16 J·mol^{-1}·K^{-1}								
$T\Delta_{\mathbf{Soln}}S^{\mathbf{Id}}$	17.60 kJ·mol^{-1}								

[a] IS: Ideal solubility. [b] Id: Ideal.

Table 5. Thermodynamic functions relative to the mixing processes of propylparaben (3) in {acetonitrile (1) + 1-propanol (2)} co-solvent mixtures at $T_{\mathrm{hm}} = 297.6$ K [a].

w_1 [b]	$\Delta_{\mathbf{mix}}G^{\circ}$ (kJ·mol^{-1})	$\Delta_{\mathbf{mix}}H^{\circ}$ (kJ·mol^{-1})	$\Delta_{\mathbf{mix}}S^{\circ}$ (J·mol^{-1} · K^{-1})	$T\Delta_{\mathbf{mix}}S^{\circ}$ (kJ·mol^{-1})
0.00	20.53	10.17	−34.81	−10.36
0.05	20.33	10.25	−33.86	−10.08
0.10	20.12	11.92	−27.58	−8.21
0.15	19.94	12.31	−25.64	−7.63
0.20	19.28	14.02	−17.68	−5.26
0.80	0.92	10.05	30.68	9.13
0.85	0.19	17.79	59.13	17.60
0.90	−0.02	19.21	64.60	19.22
0.95	0.16	17.85	59.45	17.69
1.00	0.67	13.22	42.16	12.55

[a] The average relative standard uncertainty in w_1 is $u_r(w_1) = 0.0008$. The standard uncertainty in T is $u(T) = 0.10$ K. The average relative standard uncertainties in apparent thermodynamic quantities of real dissolution processes are u_r ($\Delta_{\mathrm{mix}}G^{\circ}$) = 0.238, $u_r(\Delta_{\mathrm{mix}}H^{\circ}) = 0.028$, u_r ($\Delta_{\mathrm{mix}}S^{\circ}$) = 0.034, and $u_r(T\Delta_{\mathrm{mix}}S^{\circ}) = 0.034$. [b] w_1 is the mass fraction of acetonitrile (1) in the {acetonitrile (1) + water (2)} mixtures free of propylparaben (3).

In MeCN-rich mixtures ($0.8 \geq w_1 \leq 1.0$), the mixing Gibbs energy is close to zero and even reaches negative values ($w_1 = 0.9$), thus, cavity formation requires less energy than in water-rich mixtures. This is possibly due to the fact that W–W interactions are more energy-rich than MeCN–MeCN, and although enthalpic disfavor is observed, the process is enhanced by the entropy of mixing.

In order to evaluate the energy and organizational contribution to the mixing process, the data in Table 5 are evaluated using Perlovich's method [48,49]. Thus, in pure water, the mixing process is driven by the entropy of mixing ($T_{hm}\Delta_{\mathrm{mix}}S^{\circ} < 0; \Delta_{\mathrm{mix}}H^{\circ} > 0; |T_{hm}\Delta_{\mathrm{mix}}S^{\circ}| > |\Delta_{\mathrm{mix}}H^{\circ}|$). From $w_1 = 0.1$ up to $w_1 = 0.2$, the process is driven by the enthalpy of mixing ($T_{hm}\Delta_{\mathrm{mix}}S^{\circ} < 0; \Delta_{\mathrm{mix}}H^{\circ} > 0$). From $w_1 = 0.8$ up to $w_1 = 0.85$ and from $w_1 = 0.95$ up to pure MeCN, the mixing process is also driven by the enthalpy ($\Delta_{\mathrm{mix}}H^{\circ} > T_{hm}\Delta_{\mathrm{mix}}S^{\circ}$). Finally, in the $w_1 = 0.9$ mixture, where the maximum PP solubility is reached, the process is driven by the entropy of mixing ($\Delta_{\mathrm{mix}}H^{\circ} < T_{hm}\Delta_{\mathrm{mix}}S^{\circ}; |T_{hm}\Delta_{\mathrm{mix}}S^{\circ}| > |\Delta_{\mathrm{mix}}H^{\circ}|$).

3.4. Enthalpy–Entropy Compensation Analysis

Ryde stated that the increase in entropy is one of the consequences of non-covalent interactions between molecules, which thermodynamically disfavors the process performance. However, in order to compensate for the entropy effect, there is a simultaneous decrease in the energy factor (enthalpy) [50]. This compensation phenomenon between enthalpy and entropy produces a linear relation that allows for the evaluation of the influence of the energy (enthalpy) and organizational (entropy) factors in the process [51,52].

This relation can be evaluated by plotting $\Delta_{\mathrm{soln}}G^{\circ}$ *Vs* $\Delta_{\mathrm{soln}}H^{\circ}$, where positive slopes indicate enthalpy-driven processes and negative slopes indicate entropy-driven processes.

In this context, according to Figure 6, the process is entropy driven, since the three trends (from water up to $w_1 = 0.2$, from $w_1 = 0.8$ up to $w_1 = 0.9$ and from $w_1 = 0.9$ up to pure MeCN) have negative slopes in the case $\Delta_{soln}G^{\circ}$ *Vs* $\Delta_{soln}H^{\circ}$ (Figure 6).

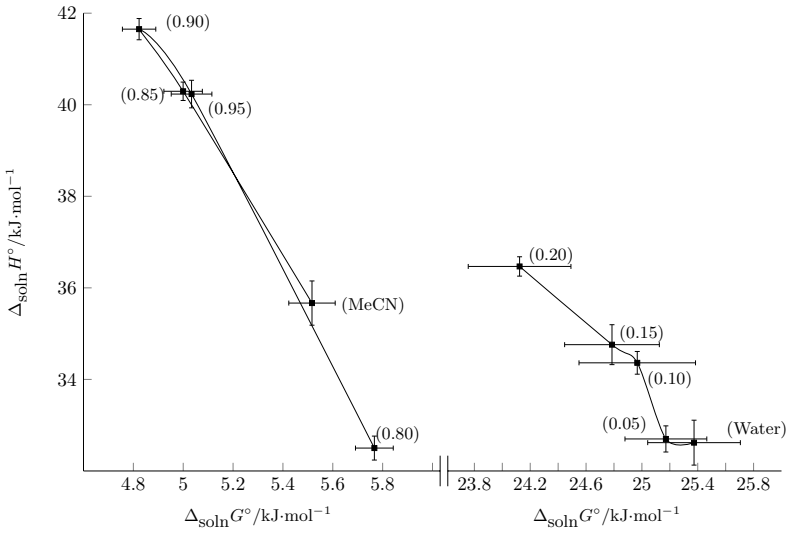

Figure 6. Enthalpy–entropy compensation plot for the solubility of propylparaben (3) in MeCN (1) + W (2) mixtures at T_{hm} = 297.6 K.

3.5. Mathematical Assessment of Solubility

One of the most versatile tools for process optimization is mathematical modeling, which allows making approximations under different conditions than experimental ones [53].

In general, the mathematical models used to correlate the drug solubility in cosolvent systems can be classified into two groups. In the first group, there are models that allow correlating the solubility as a function of the cosolvent composition, and the most commonly used models are Yalkowsky–Roseman [7,54], Wilson [55], Modifyed Wilson [56], NRTL [57] and Extended Hildebrand [29,58]. In the second group are the models that correlate solubility as a function of temperature; these models, in addition to allowing correlation of solubility data, have an important predictive potential as long as the data to be predicted are interpolated. In the last, the most commonly used models are va not Hoff [19], Apelblat [59] and Buchowski–Ksiazaczak λh [60].

Since PP exhibits liquid phase separation in intermediate mixtures, models that correlate solubility as a function of cosolvent composition cannot be used; therefore, models whose independent variable is temperature were used.

Accordingly, the experimental solubility data (Table 1) were correlated with the models proposed by va not Hoff (Equation (10)), Apelblat (Equation (11)) and Buchowski–Ksiazaczak λh (Equation (12)),

$$\ln x_3 = A + \frac{B}{T} \tag{10}$$

$$\ln x_3 = A + \frac{B}{T} + C \ln T \tag{11}$$

$$\ln\left[1 + \frac{\lambda(1 - x_3)}{x_3}\right] = \lambda h\left[\frac{1}{T} - \frac{1}{T_m}\right] \tag{12}$$

where x_3 is the calculated solubility; A, B, C, λ and h are model-specific parameters; T is the study temperature; and T_m is the PP melting temperature.

The model equation parameters assessed and the average relative deviation (ARD) (Equation (13)) are presented in Tables 6–8.

$$ARD = \frac{100}{N}\sum_{i=1}^{N}\left|\frac{x_3 - x_3^{cal}}{x_3}\right| \quad (13)$$

where N is the number of solubility data points, and x_3 and x_3^{cal} represent the experimentally measured and calculated solubility, respectively.

Table 6. The va not Hoff model parameters.

w_1 [a]	A	B	ARD [b]
0.00	3.56 ± 0.36	−4116.30 ± 111.63	3.79
0.05	3.22 ± 0.32	−3987.13 ± 99.51	2.07
0.10	3.73 ± 0.11	−4112.51 ± 33.57	1.30
0.15	4.52 ± 0.33	−4330.91 ± 101.26	3.43
0.20	4.91 ± 0.10	−4362.04 ± 30.01	1.21
0.80	10.82 ± 0.27	−3913.52 ± 83.91	1.49
0.85	14.00 ± 0.33	−4770.38 ± 101.79	2.30
0.90	14.72 ± 0.24	−4958.96 ± 73.08	1.33
0.95	14.31 ± 0.13	−4858.76 ± 40.13	0.99
1.00	12.63 ± 0.51	−4424.53 ± 158.78	4.17
Overall ARD			2.08

[a] w_1 is the mass fraction of MeCN (1) in the {MeCN (1) + W (2)} mixtures free of propylparaben (3). [b] The average relative deviation (ARD).

Table 7. The Apelblat model parameters.

w_1 [a]	A	B	C	ARD [b]
0.00	−0.052 ± 0.004	2.174 ± 0.177	0.008 ± 0.001	3.70
0.05	−0.049 ± 0.005	2.035 ± 0.232	0.007 ± 0.001	4.01
0.10	−0.054 ± 0.003	2.255 ± 0.121	0.008 ± 0.0	1.85
0.15	−0.07 ± 0.007	2.916 ± 0.329	0.01 ± 0.001	3.81
0.20	−0.087 ± 0.006	3.608 ± 0.246	0.013 ± 0.001	3.18
0.80	−116.6 ± 10.0	4835.8 ± 444.1	17.636 ± 1.494	3.21
0.85	−235.6 ± 16.1	9871.4 ± 713.2	35.57 ± 2.399	4.14
0.90	−280.3 ± 18.1	11771.6 ± 802.1	42.288 ± 2.698	4.73
0.95	−251.8 ± 17.1	10576.2 ± 757.7	37.992 ± 2.548	4.41
1.00	−174.6 ± 22.5	7322.6 ± 998.7	26.346 ± 3.359	5.01
Overall ARD				3.81

[a] w_1 is the mass fraction of MeCN (1) in the {MeCN (1) + W (2)} mixtures free of propylparaben (3). [b] The average relative deviation (ARD).

Table 8. The Buchowski–Ksiazaczak λh model parameters.

w_1 [a]	λ	h	ARD [b]
0.00	$0.0003 \pm 2{\cdot}10^{-5}$	11,301,162 ± 525,076	2.97
0.05	$0.0003 \pm 2{\cdot}10^{-5}$	10,420,554 ± 353,844	2.01
0.10	$0.0004 \pm 2{\cdot}10^{-5}$	8,606,763 ± 278,840	1.88
0.15	$0.0005 \pm 3{\cdot}10^{-5}$	7,765,353 ± 348,425	2.62
0.20	$0.0008 \pm 3{\cdot}10^{-5}$	5,352,830 ± 161,122	1.72
0.80	1.42 ± 0.08	2846.3 ± 101.3	1.60
0.85	5.83 ± 0.46	954.6 ± 55.6	3.06
0.90	8.31 ± 0.76	714.0 ± 49.5	3.81
0.95	6.10 ± 0.51	919.4 ± 57.4	2.90
1.00	2.49 ± 0.27	1877.5 ± 150.7	4.55
Overall ARD			2.71

[a] w_1 is the mass fraction of MeCN (1) in the {MeCN (1) + W (2)} mixtures free of propylparaben (3). [b] The average relative deviation (ARD).

The data calculated using the three mathematical models are well-correlated with the experimental data. Thus, the va not Hoff model is the best correlated with an ARD of 2.2, and the Apelblat model has the highest dispersion with an ARD of 3.8. Figure 7 shows the correlation between the experimental and calculated data, obtaining r^2 values greater than 0.99, validating the results obtained through the ARD analysis and confirming that the three models are well-correlated, considering that a model is useful if it reports ARD values below 30.0 [61,62].

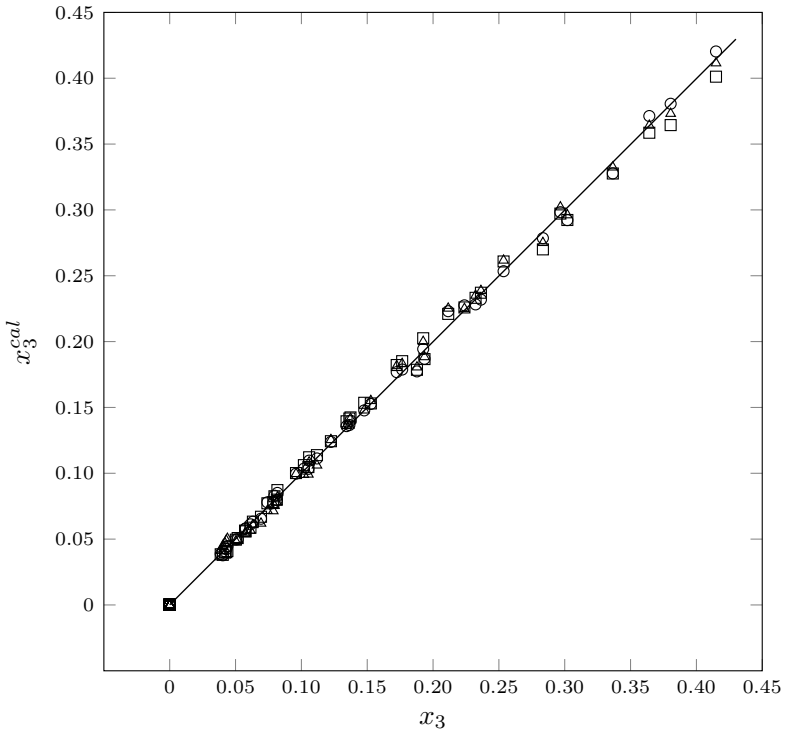

Figure 7. The experimental solubility data versus predicted solubility of PP (3) in {MeCN (1) + W (2)} cosolvent mixtures (○ = va not Hoff (r^2 = 997); △: Apelblat (r^2 = 992) and □: Buchowski–Ksiazaczak λh model (r^2 = 995).

4. Conclusions

The PP solubility in cosolvent mixtures {MeCN (1) + W (2)} is an endothermic process that is dependent on the cosolvent composition. In intermediate mixtures, liquid phase separation occurs, possibly due to a higher affinity of PP for one of the solvents that form the cosolvent mixture. In addition, the mixture {MeCN (1) + W (2)} presents microheterogeneity in intermediate mixtures, which would also favor the separation of liquid phases.

The Gibbs energy of the solution is positive in all cases and lower in MeCN-rich mixtures due to a higher solubility of PP with these mixtures. Regarding the enthalpy and entropy of the solution, they are positive in all cases. This indicates an enthalpic depletion compensated by an entropic enhancement that allows the development of the solution process.

Finally, the PP experimental solubility is well-correlated with the va not Hoff, Apelblat and Buchowski–Ksiazaczak λh models with ARD values below 4.0.

Author Contributions: Conceptualization, C.P.O. and D.R.D.; methodology, D.R.D. and C.P.O.; software, R.E.C.-T.; validation, C.P.O. and D.R.D.; formal analysis, C.P.O.; investigation, M.H. and C.P.O.; resources, M.H. and D.R.D.; data curation, D.R.D.; writing—original draft preparation, C.P.O.; writing—review and editing, M.H., C.P.O. and D.R.D.; visualization, C.P.O.; supervision, D.R.D.; project administration, D.R.D.; and funding acquisition, D.R.D. All authors have read and agreed to the published version of the manuscript.

Funding: This research was funded by Universidad Cooperativa de Colombia grant number INV2976.

Institutional Review Board Statement: Not applicable for studies not involving humans or animals.

Informed Consent Statement: Not applicable for studies not involving humans.

Data Availability Statement: Data are contained within the article.

Acknowledgments: We thank the National Directorate of Research and National Committee for Research Development of the Universidad Cooperativa de Colombia for the financial support of the Project "Análisis matemático y termodinámico de la solubilidad algunas sustancias antimicrobianas de uso industrial en mezclas cosolventes" with code INV2976. We also thank the Universidad Cooperativa de Colombia, Sede Neiva for facilitating the laboratories and equipment used.

Conflicts of Interest: The authors declare no conflict of interest.

Abbreviations

The following abbreviations are used in this manuscript:

C_P	Molar heat capacity
CAS	Chemical Abstracts Service Registry Number
DSC	Differential scanning calorimetry
g	grams
G	Gibbs Energy
GC	Gas Chromatography
H	Enthalpy
hm	Harmonic mean
HPLC	High Performance Liquid Chromatography
id	Ideal
J	Joule
K	Kelvin
k	kilo
m	Melting
MeCN	Acetonitrile
mix	Mixing
PEG	Polyethylene glycol 200
PP	Propylparaben
R	Gas constant
S	Entropy
sol	Solution
tr	Transfer
T	Temperature
T_{hm}	Harmonic temperature
UV	Ultraviolet
W	Water
w	Mass fraction
x	Mole fraction
δ	Solubility parameter
$XRPD$	X-ray powder diffraction

References

1. Shahvar, A.; Soltani, R.; Saraji, M.; Dinari, M.; Alijani, S. Covalent triazine-based framework for micro solid-phase extraction of parabens. *J. Chromatogr. A* **2018**, *1565*, 48–56. [CrossRef]
2. Han, J.H.; Cui, Y.Y.; Yang, C.X. Tailored amino/hydroxyl bifunctional microporous organic network for efficient stir bar sorptive extraction of parabens and flavors from cosmetic and food samples. *J. Chromatogr. A* **2021**, *1655*, 462521. [CrossRef]
3. Yang, X.S.; Wang, L.L.; Liu, Y.S.; Yang, C.X.; Zhao, J.; Ji, S.L.; Liu, Q.W.; Hu, Z.H.; Liu, F.J.; Wang, P. Fabrication of magnetic covalent organic framework for effective and selective solid-phase extraction of propylparaben from food samples. *Food Chem.* **2022**, *386*, 132843. [CrossRef] [PubMed]
4. Cárdenas, Z.J.; Jiménez, D.M.; Delgado, D.R.; Almanza, O.A.; Jouyban, A.; Martínez, F.; Acree, W.E. Solubility and preferential solvation of some n-alkyl-parabens in methanol+water mixtures at 298.15 K. *J. Chem. Thermodyn.* **2017**, *108*, 26–37. [CrossRef]

5. Rudyanto, M.; Ihara, M.; Takasu, K.; Yoshida, M.; Poerwono, H.; Sudiana, I.K.; Indrayanto, G.; Brittain, H.G. Propylparaben: Physical Characteristics. In *Profiles of Drug Substances, Excipients and Related Methodology*; Academic Press: Cambridge, MA, USA, 2003; Volume 30, pp. 235–269. [CrossRef]
6. Jouyban, A. *Handbook of Solubility Data for Pharmaceuticals*; CRC Press: Boca Raton, FL, USA, 2010.
7. Yalkowsky, S.H. *Solubility and Solubilization in Aqueous Media*; American Chemical Society: Washington, DC, USA, 1999.
8. Sinko, P.; Martin, A. *Martin's Physical Pharmacy and Pharmaceutical Sciences: Physical Chemical and Biopharmaceutical Principles in the Pharmaceutical Sciences*; Lippincott Williams & Wilkins: Philadelphia, PA, USA, 2006.
9. Trujillo-Trujillo, C.F.; Angarita-Reina, F.; Herrera, M.; Ortiz, C.P.; Cardenas-Torres, R.E.; Martinez, F.; Delgado, D.R. Thermodynamic Analysis of the Solubility of Sulfadiazine in (Acetonitrile 1-Propanol) Cosolvent Mixtures from 278.15 K to 318.15 K. *Liquids* **2023**, *3*, 7–18. [CrossRef]
10. Torres-Cardozo, A.; Cerquera, N.E.; Ortiz, C.P.; Osorio-Gallego, J.; Cardenas-Torres, R.E.; Angarita-Reina, F.; Martinez, F.; Delgado, D.R. Thermodynamic analysis of the solubility of progesterone in 1-octanol + ethanol cosolvent mixtures at different temperatures. *Alex. Eng. J.* **2023**, *64*, 219–235. [CrossRef]
11. Zhao, Y.; Zada, A.; Yang, Y.; Pan, J.; Wang, Y.; Yan, Z.; Xu, Z.; Qi, K. Photocatalytic Removal of Antibiotics on g-C3N4 Using Amorphous CuO as Cocatalysts. *Front. Chem.* **2021**, *9*, 797738. [CrossRef]
12. Liu, S.; Zada, A.; Yu, X.; Liu, F.; Jin, G. NiFe2O4/g-C3N4 heterostructure with an enhanced ability for photocatalytic degradation of tetracycline hydrochloride and antibacterial performance. *Chemosphere* **2022**, *307*, 135717. [CrossRef]
13. Yue, D.; William, E.A., Jr.; Abraham, M.H. Applications of Abraham solvation parameter model: Estimation of the lethal median molar concentration of the antiepileptic drug levetiracetam towards aquatic organisms from measured solubility data. *Phys. Chem. Liq.* **2020**, *58*, 302–308. [CrossRef]
14. Liu, X.; Abraham, M.H.; William, E.A., Jr. Abraham Model Descriptors for Melatonin; Prediction of Solution, Biological and Thermodynamic Properties. *J. Solut. Chem.* **2022**, *51*, 992–999. [CrossRef]
15. van Oss, C.J. *Interfacial Forces in Aqueous Media*, 2nd ed.; CRC Press: Boca Raton, FL, USA, 2006.
16. Rubino, J.; Yalkowsky, S. Cosolvency and cosolvent polarity. *Pharm. Res.* **1987**, *4*, 220–230. [CrossRef] [PubMed]
17. Cárdenas, Z.J.; Jiménez, D.M.; Rodríguez, G.A.; Delgado, D.R.; Martínez, F.; Khoubnasabjafari, M.; Jouyban, A. Solubility of methocarbamol in some cosolvent+water mixtures at 298.15 K and correlation with the Jouyban–Acree model. *J. Mol. Liq.* **2013**, *188*, 162–166. [CrossRef]
18. Rubino, J.T. Cosolvents and Cosolvency. In *Encyclopedia of Pharmaceutical Science and Technology*, 4th ed.; Swarbrick, J., Ed.; CRC Press: Boca Raton, FL, USA, 2015; pp. 61–73.
19. Romero-Nieto, A.M.; Caviedes-Rubio, D.I.; Polania-Orozco, J.; Cerquera, N.E.; Delgado, D.R. Temperature and cosolvent composition effects in the solubility of methylparaben in acetonitrile + water mixtures. *Phys. Chem. Liq.* **2020**, *58*, 722–735. [CrossRef]
20. Romero-Nieto, A.M.; Cerquera, N.E.; Martínez, F.; Delgado, D.R. Thermodynamic study of the solubility of ethylparaben in acetonitrile + water cosolvent mixtures at different temperatures. *J. Mol. Liq.* **2019**, *287*, 110894. [CrossRef]
21. Dittert, L.W.; Higuchi, T.; Reese, D.R. Phase solubility technique in studying the formation of complex salts of triamterene. *J. Pharm. Sci.* **1964**, *53*, 1325–1328. [CrossRef]
22. Mader, W.J.; Higuchi, T. Phase solubility analysis. *C R C Crit. Rev. Anal. Chem.* **1970**, *1*, 193–215. [CrossRef]
23. Higuchi, T.; Connors, K. *Advances in Analytical Chemistry and Instrumentation*; Interscience Publishers, Inc.: New York, NY, USA, 1965.
24. Koley, S.; Ghosh, S. Study of Microheterogeneity in Acetonitrile–Water Binary Mixtures by using Polarity-Resolved Solvation Dynamics. *ChemPhysChem* **2015**, *16*, 3518–3526. [CrossRef]
25. Marcus, Y. The structure of and interactions in binary acetonitrile + water mixtures. *J. Phys. Org. Chem.* **2012**, *25*, 1072–1085. [CrossRef]
26. Paruta, A.N. Solubility of the Parabens in Dioxane—Water Mixtures. *J. Pharm. Sci.* **1969**, *58*, 204–206. [CrossRef]
27. Paruta, A.N.; Sciarrone, B.J.; Lordi, N.G. Solubility profiles for the xanthines in dioxane—water mixtures. *J. Pharm. Sci.* **1965**, *54*, 838–841. [CrossRef]
28. Peña, M.A.; Bustamante, P.; Escalera, B.; Reíllo, A.; Bosque-Sendra, J.M. Solubility and phase separation of benzocaine and salicylic acid in 1,4-dioxane–water mixtures at several temperatures. *J. Pharm. Biomed. Anal.* **2004**, *36*, 571–578. [CrossRef]
29. Hildebrand, J. *Regular and Related Solutions: The Solubility of Gases, Liquids and Solids*; Van Nostrand Reinhold: New York, NY, USA, 1970.
30. Alexander, K.; Laprade, B.; Mauger, J.; Paruta, A.N. Thermodynamics of Aqueous Solutions of Parabens. *J. Pharm. Sci.* **1978**, *67*, 624–627. [CrossRef]
31. Prankerd, R. Solid-state properties of drugs. I. Estimation of heat capacities for fusion and thermodynamic functions for solution from aqueous solubility-temperature dependence measurements. *Int. J. Pharm.* **1992**, *84*, 233–244. [CrossRef]
32. Yang, H.; Rasmuson, A.C. Ternary phase diagrams of ethyl paraben and propyl paraben in ethanol aqueous solvents. *Fluid Phase Equilibria* **2014**, *376*, 69–75. [CrossRef]
33. Ouyang, J.; Chen, J.; Zhou, L.; Liu, Z.; Zhang, C. Solubility Measurement, Modeling, and Dissolution Thermodynamics of Propylparaben in 12 Pure Solvents. *J. Chem. Eng. Data* **2020**, *65*, 4725–4734. [CrossRef]

34. Yang, H.; Svärd, M.; Zeglinski, J.; Rasmuson, A.C. Influence of Solvent and Solid-State Structure on Nucleation of Parabens. *Cryst. Growth Des.* **2014**, *14*, 3890–3902. [CrossRef]
35. Martin, A.; Carstensen, J. Extended Solubility Approach: Solubility Parameters for Crystalline Solid Compounds. *J. Pharm. Sci.* **1981**, *70*, 170–172. [CrossRef]
36. Perlovich, G.L.; Rodionov, S.V.; Bauer-Brandl, A. Thermodynamics of solubility, sublimation and solvation processes of parabens. *Eur. J. Pharm. Sci.* **2005**, *24*, 25–33. [CrossRef]
37. Giordano, F.; Bettini, R.; Donini, C.; Gazzaniga, A.; Caira, M.R.; Zhang, G.G.; Grant, D.J. Physical properties of parabens and their mixtures: Solubility in water, thermal behavior, and crystal structures. *J. Pharm. Sci.* **1999**, *88*, 1210–1216. [CrossRef]
38. Krug, R.R.; Hunter, W.G.; Grieger, R.A. Enthalpy-entropy compensation. 1. Some fundamental statistical problems associated with the analysis of va not Hoff and Arrhenius data. *J. Phys. Chem.* **1976**, *80*, 2335–2341. [CrossRef]
39. Krug, R.R.; Hunter, W.G.; Grieger, R.A. Enthalpy-entropy compensation. 2. Separation of the chemical from the statistical effect. *J. Phys. Chem.* **1976**, *80*, 2341–2351. [CrossRef]
40. Aydi, A.; Dali, I.; Ghachem, K.; Al-Khazaal, A.Z.; Delgado, D.R.; Kolsi, L. Solubility of Hydroxytyrosol in binary mixture of ethanol + water from (293.15 to 318.15) K: Measurement, correlation, dissolution thermodynamics and preferential solvation. *Alex. Eng. J.* **2021**, *60*, 905–914. [CrossRef]
41. Cárdenas-Torres, R.E.; Ortiz, C.P.; Acree, W.E.; Jouyban, A.; Martínez, F.; Delgado, D.R. Thermodynamic study and preferential solvation of sulfamerazine in acetonitrile + methanol cosolvent mixtures at different temperatures. *J. Mol. Liq.* **2022**, *349*, 118172. [CrossRef]
42. Agredo-Collazos, J.J.; Ortiz, C.P.; Cerquera, N.E.; Cardenas-Torres, R.E.; Peña, M.A.; Martínez, F. Equilibrium Solubility of Triclocarban in (Cyclohexane + 1,4-Dioxane) Mixtures: Determination, Correlation, Thermodynamics and Preferential Solvation. *J. Solut. Chem.* **2022**, *51*, 1603–1625. [CrossRef]
43. Yalkowsky, S.H.; Wu, M. Estimation of the ideal solubility (crystal-liquid fugacity ratio) of organic compounds. *J. Pharm. Sci.* **2010**, *99*, 1100–1106. [CrossRef] [PubMed]
44. Neau, S.H.; Flynn, G.L. Solid and Liquid Heat Capacities of n-Alkyl Para-aminobenzoates Near the Melting Point. *Pharm. Res.* **1990**, *7*, 157–1162. [CrossRef]
45. Neau, S.H.; Bhandarkar, S.V.; Hellmuth, E.W. Differential Molar Heat Capacities to Test Ideal Solubility Estimations. *Pharm. Res.* **1997**, *14*, 601–605. [CrossRef]
46. Opperhuizen, A.; Gobas, F.A.P.C.; Van der Steen, J.M.D.; Hutzinger, O. Aqueous solubility of polychlorinated biphenyls related to molecular structure. *Environ. Sci. Technol.* **1988**, *22*, 638–646. [CrossRef]
47. Delgado, D.R.; Mogollon-Waltero, E.M.; Ortiz, C.P.; Peña, M.A.; Almanza, O.A.; Martínez, F.; Jouyban, A. Enthalpy-entropy compensation analysis of the triclocarban dissolution process in some {1,4-dioxane (1) + water (2)} mixtures. *J. Mol. Liq.* **2018**, *271*, 522–529. [CrossRef]
48. Perlovich, G.L.; Tkachev, V.V.; Strakhova, N.N.; Kazachenko, V.P.; Volkova, T.V.; Surov, O.V.; Schaper, K.; Raevsky, O.A. Thermodynamic and structural aspects of sulfonamide crystals and solutions. *J. Pharm. Sci.* **2009**, *98*, 4738–4755. [CrossRef]
49. Perlovich, G.L.; Strakhova, N.N.; Kazachenko, V.P.; Volkova, T.V.; Tkachev, V.V.; Schaper, K.J.; Raevsky, O.A. Sulfonamides as a subject to study molecular interactions in crystals and solutions: Sublimation, solubility, solvation, distribution and crystal structure. *Int. J. Pharm.* **2008**, *349*, 300–313. [CrossRef]
50. Ryde, U. A fundamental view of enthalpy–entropy compensation. *RSC Med. Chem.* **2014**, *5*, 1324–1336. [CrossRef]
51. Sharp, K. Entropy—enthalpy compensation: Fact or artifact? *Protein Sci.* **2001**, *10*, 661–667. [CrossRef]
52. Chodera, J.D.; Mobley, D.L. Entropy-Enthalpy Compensation: Role and Ramifications in Biomolecular Ligand Recognition and Design. *Annu. Rev. Biophys.* **2013**, *42*, 121–142. [CrossRef]
53. Delgado, D.R.; Peña, M.A.; Martínez, F. Extended Hildebrand solubility approach applied to sulphadiazine, sulphamerazine and sulphamethazine in some 1-propanol (1) + water (2) mixtures at 298.15 K. *Phys. Chem. Liq.* **2019**, *57*, 388–400. [CrossRef]
54. Vargas-Santana, M.S.; Cruz-González, A.M.; Cerquera, N.E.; Escobar Rodriguez, A.S.; Cardenas, R.E.; Calderón-Losada, O.; Ortiz, C.P.; Delgado, D.R. Método extendido de Hildebrand y modelo de Yalkowsky- Roseman en la estimación de la solubilidad de sulfadiazina y sulfametazina en algunas mezclas etilenglicol (1) + agua (2) a varias temperaturas. *Rev. Colomb. De Cienc. Químico-Farm.* **2022**, *50*, 812–836. [CrossRef]
55. Cárdenas, R.E.; Tinoco, L.E.; Galindres, D.M.; Beltrán, A.; Oviedo, C.D.; Osorio, J. Predicción de la solubilidad de la sulfadiazina en algunas mezclas cosolventes utilizando modelos de solución no ideales. *Rev. Colomb. De Cienc. Químico-Farm.* **2020**, *49*, 822–842. [CrossRef]
56. Tinoco, L.E.; Galindres, D.M.; Osorio, J.; Cárdenas, R.E. Predicción de la solubilidad de sulfamerazina y sulfametazina en algunas mezclas cosolventes utilizando modelos de solución no ideales. *Rev. Colomb. De Cienc. Químico-Farm.* **2021**, *50*, 292–313. [CrossRef]
57. Renon, H.; Prausnitz, J.M. Local compositions in thermodynamic excess functions for liquid mixtures. *AIChE J.* **1968**, *14*, 135–144. [CrossRef]
58. Sotomayor, R.G.; Holguín, A.R.; Cristancho, D.M.; Delgado, D.R.; Martínez, F. Extended Hildebrand Solubility Approach applied to piroxicam in ethanol+water mixtures. *J. Mol. Liq.* **2013**, *180*, 34–38. [CrossRef]
59. Blokhina, S.V.; Ol'khovich, M.V.; Sharapova, A.V.; Levshin, I.B.; Perlovich, G.L. Thermodynamic insights to solubility and lipophilicity of new bioactive hybrids triazole with thiazolopyrimidines. *J. Mol. Liq.* **2021**, *324*, 114662. [CrossRef]

60. Ksiazczak, A.; Kosinski, J.J. Vapour pressure of binary, three-phase (S-L-V) systems and solubility. *Fluid Phase Equilibria* **1988**, *44*, 211–236. [CrossRef]
61. Jouyban, A. Review of the cosolvency models for predicting solubility of drugs in water-cosolvent mixtures. *J. Pharm. Pharm. Sci.* **2008**, *11*, 32–58. [CrossRef] [PubMed]
62. Jouyban, A.; Acree, W.E. Mathematical derivation of the Jouyban-Acree model to represent solute solubility data in mixed solvents at various temperatures. *J. Mol. Liq.* **2018**, *256*, 541–547. [CrossRef]